Journal of Magnetism and Magnetic Materials 393 (2015) 82–87

Contents lists available at ScienceDirect

Journal of Magnetism and Magnetic Materials

journal homepage: www.elsevier.com/locate/jmmm

Impact of silica-coating on the microwave absorption properties of carbonyl iron powder

J. Li [b], W.J. Feng [a,b,*], J.S. Wang [b], X. Zhao [b], W.Q. Zheng [b], H. Yang [a,b]

[a] State Key Laboratory of Advanced Processing and Recycling of Nonferrous Metal, Lanzhou University of Technology, Lanzhou 730050, China
[b] School of Science, Lanzhou University of Technology, Lanzhou, Gansu 730050, China

ARTICLE INFO

Article history:
Received 25 January 2015
Received in revised form
14 May 2015
Accepted 17 May 2015
Available online 19 May 2015

Keywords:
Electromagnetic wave absorption
CIP
Coating layer
Complex permittivity and complex permeability
The tangents of loss angles
Reflection loss

ABSTRACT

Microwave absorption properties, especially the band width and depth of reflection loss are highlighted as key measurement in studies of microwave absorber. In order to improve the band width and depth of reflection loss of carbonyl iron powder (CIP), we prepared SiO_2 layers on the surface of CIP by using tetraethyl orthosilicate (TEOS) as a SiO_2 source and 3-aminopropyl triethoxysilane (APTES) as a surface modifier. SiO_2 layer was formed by the hydrolysis of TEOS. The results show that after treatment the CIP is covered by a 5–10 nm coating layer. Contrast to uncoated samples, coated samples show improved absorption properties. The minimum of reflection loss is −38.8 dB at 11 GHz and the band width of reflection loss exceeding −10 dB is from 8 GHz to 14 GHz.

1. Introduction

The application of wave-absorbing material is the effective way to alleviate the increasingly serious electromagnetic wave pollution [1–4]. Carbonyl iron powder is one of the common wave-absorbing materials. It is hoped that through the modification of carbonyl iron powder to further strengthen its effective absorbing bandwidth and the strength of the wave-absorbing [5–7]. Common modification methods include, transform the microstructure of CIP through ball-milling or altering the preparation conditions and so on [8,9], composite the CIP with other materials by methods as coating, etc [10–15].

In previous studies, the CIP@SiO_2 was proved to be an effective means of modification [16, 17]. As the Reference [16], the author put polyvinylpyrrolidone as surface modifying agent, and TEOS as silicon source for preparing CIP@SiO_2 TEOS, the bandwidth of the reflection loss which is less than −8 dB achieved 10 GHz; In reference [17], the author prepared CIP@SiO_2 by drying and dehydration of silica solution, the bandwidth of the reflection loss which is less than −10 dB achieved 3.8 GHz. But both references are lack of convictive analysis about the absorbing mechanism of CIP@SiO_2.

In this study, a SiO_2 coating layer is prepared on the CIP surface by chemical bath deposition of APTES and TEOS in the ethanol-water solution. The CIP@SiO_2 was prepared via this method and applied for wave-absorbing material that is a first try. In addition,

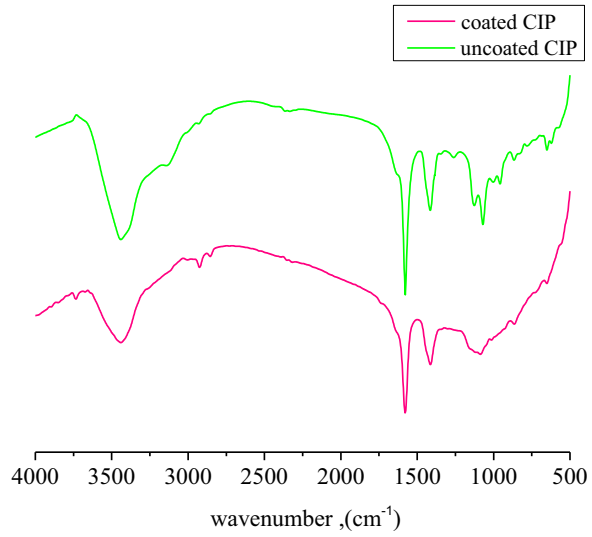

Fig.1. The infrared absorption spectroscopy of the coated sample and uncoated sample.

* Corresponding author at: School of Science, Lanzhou University of Technology, Lanzhou, Gansu 730050, China.
E-mail address: wjfeng@lut.cn (W.J. Feng).

http://dx.doi.org/10.1016/j.jmmm.2015.05.049
0304-8853/

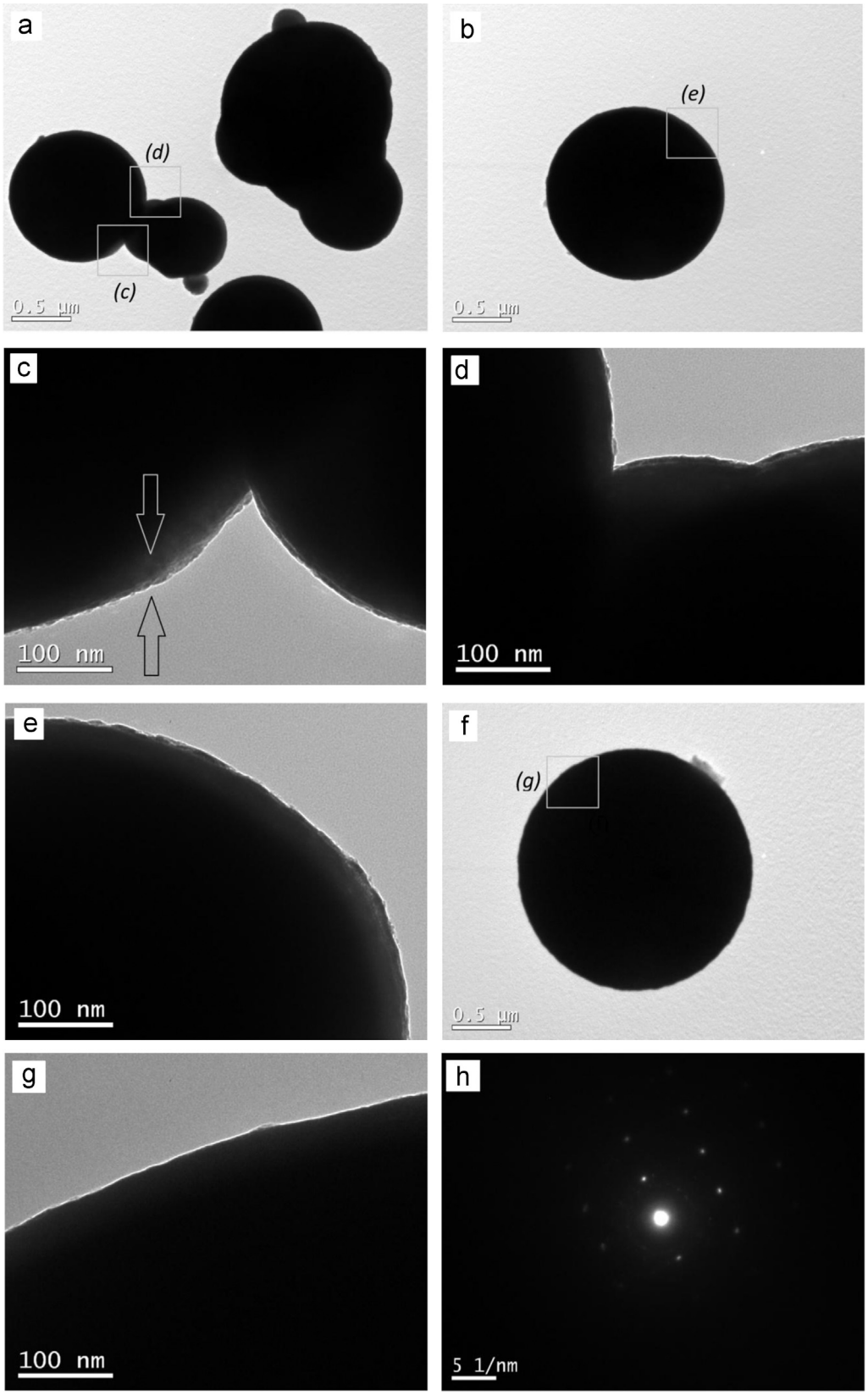

Fig. 2. (a) and (b) are the TEM photos of the coated powder ($x=3$) under low magnification, (c)–(e) are the TEM photos of the coated powder ($x=3$) under high magnification, (f) and (g) are the TEM photos of the uncoated powder (f is under low magnification), (h) is the pattern of electron diffraction of coated powder.

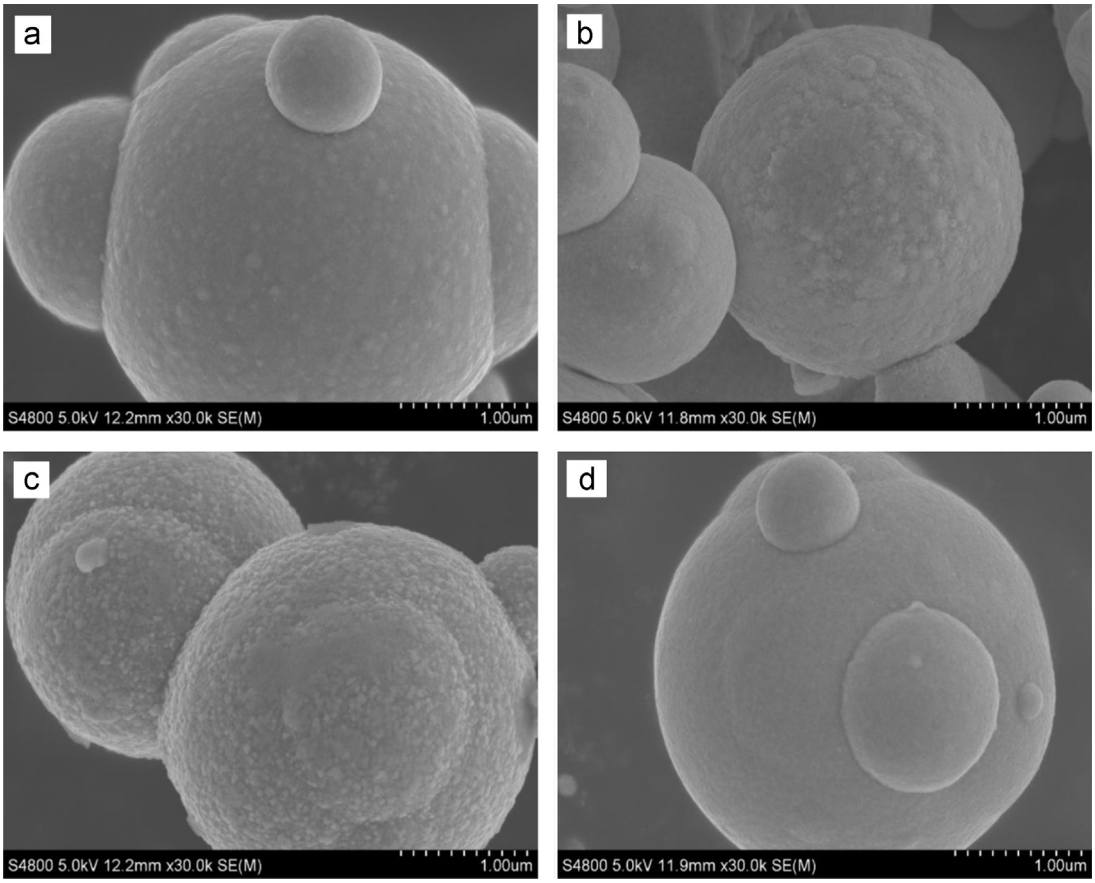

Fig.3. the SEM photos of the coated powder (a) $x=2$ (b) $x=3$ (c) $x=8$ and uncoated powder (d).

this study makes the analysis and discussion of the wave-absorbing mechanism of CIP@SiO_2.

2. Experimental method and material characterization

CIP used in this experiment was purchased from Tianyi metal particle CO. (the average particle size is 7 μm). TEOS APTES and anhydrous ethanol were AR.

The coatings were fabricated in the following method. Firstly, TEOS and APTES were dissolved in ethanol by the volume ratio of 1: x: 2400 (APTES: TEOS: ethanol, $x=2$, 3, 4, 8). Then CIP was mixed with Di-water, typically, 1 g CIP in 100 ml. The mixture was stirred to be suspended and poured into the ethanol solution mentioned above. The mixed solution was set in a constant temperature water bath (40 °C) and stirred by electric mixer (500 r/min) for 3 h. After drying grinding and washing, powder samples were obtained. The chemical reaction can be expressed by the following formulas [18]:

$$(C_2H_5O)_4Si + 4H_2O \rightarrow Si(OH)_4 + 4C_2H_5OH$$

$$Si(OH)_4 \rightarrow SiO_2 + H_2O$$

APTES was known as a silane coupling agent, and here was used as a surface modifier. Because of its strong polar group—amino, it can form a monomolecular layer on the surface of CIP by polar absorption. Its non-polar group can build Si–O bond during hydrolysis, and absorb SiO_2 which is produced by the hydrolysis of TEOS, then forms a SiO_2coating layer on the surface of CIP.

Powder samples were mixed with melted paraffin (4:1 in mass), and poured into the mold which had a 3.02 mm inner diameter and a 7.00 mm outer diameter. The sample was made in the shape of a hollow column. The height was between 4–6 mm.

The morphologies of samples were characterized by a JSM-6700F Field emission scanning electron microscope and a http://sklab.lut.cn/www/ContentsDisp.asp?id=118&ClassId=31JEM-2010 transmission electron microscope. The infrared absorption spectroscopy of samples was measured by an FT-Roman Module Raman spectrometer. The electromagnetic parameters of the hollow column samples were measured by an Agilent/HP-8720ET Vector Network Analyzer.

3. Results and discussion

3.1. Component analysis and morphological properties

Fig.1 exhibits the infrared absorption spectroscopy of the samples ($x=3$ and an uncoated sample). The curve of the coated sample shows a wide absorbing peak around 1100 cm^{-1}which refers to antisymmetric vibration mode of Si–O–Si bond and is a characteristic peak of quartz class mineral [19]. The changes of absorbing peak can prove the existence of SiO_2in the samples.

Fig.2 shows the TEM images of CIP coated by SiO_2. The marked part in (c) shows different transparency with the other part of the particle. In consideration of the high conductivity and high density of iron, the image of CIP on TEM photos should be dark and uniform, like what is shown in (f) and (g) which were taken from an uncoated sample. Combined with the result of the infrared absorption spectroscopy, the marked area in (c) is the SiO_2 coating layer which is 5–10 nm on thickness approximately. From (c)–(e), we could see that the SiO_2 coating layers have covered the surface of CIP entirely. (h) Shows the pattern of electron diffraction of

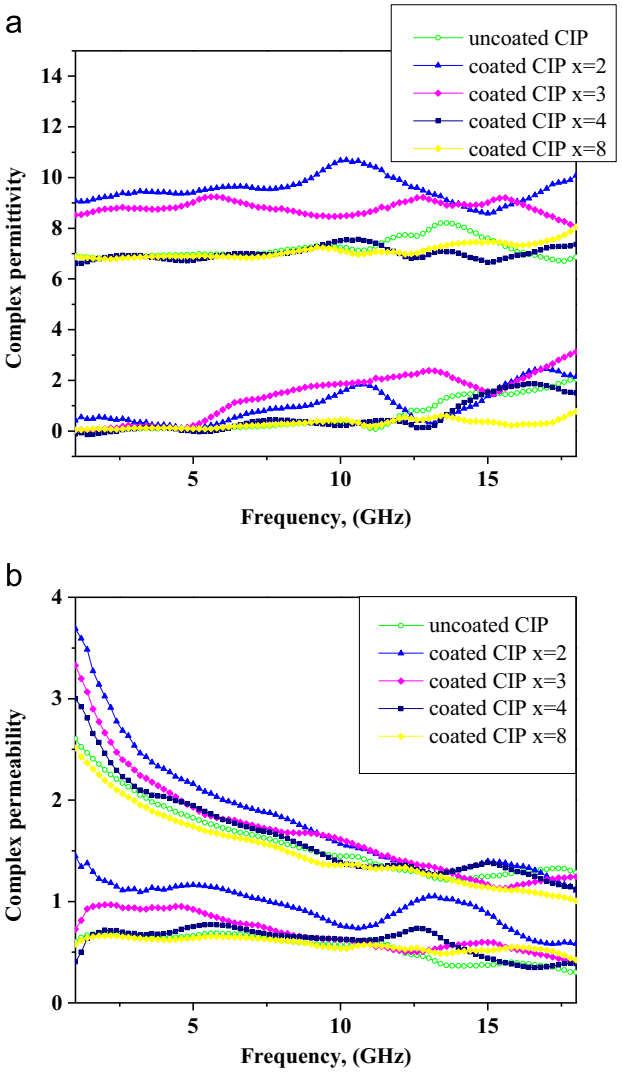

Fig.4. complex permittivity and permeability of samples (uncoated CIP, coated CIP $x=2$ $x=3$ $x=4$ and $x=8$).

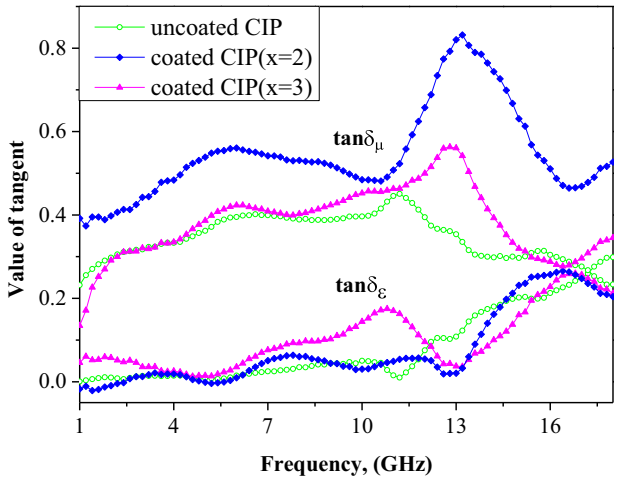

Fig.5. The tangents of loss angles (uncoated CIP, coated CIP $x=2$ $x=3$).

coated powder. The pattern matches the fcc structure well, which is the typical structure of α-Fe.

The SEM photos of the coated and uncoated powder are shown in Fig.3. It is shown that an island-shaped distribution coating

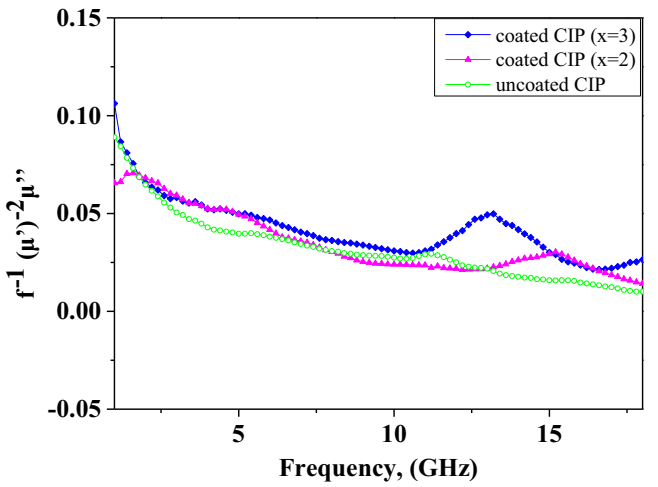

Fig.6. the values of $f^{-1}(\mu')^{-2}\mu''$ varied with frequency (uncoated CIP, coated CIP $x=2$, coated CIP $x=3$).

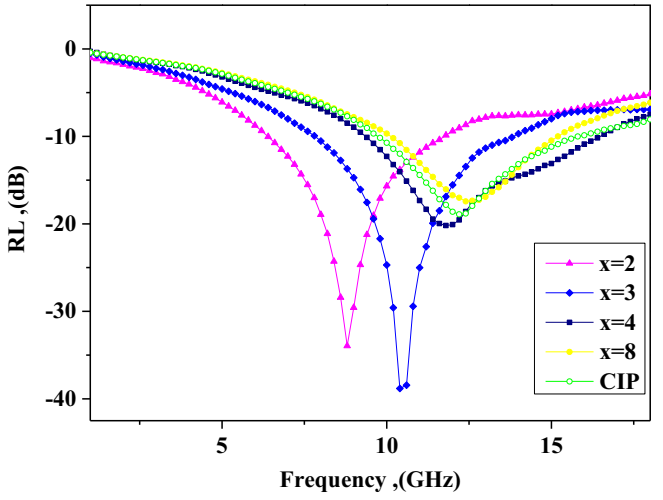

Fig.7. (a) is RL curves of samples when d is 1.9 mm; (b) is RL curves of coated sample ($x=3$) in different values of d.

Table 1
the EM absorption properties of some recent reports.

Materials	RL lower than −20 dB	The min of RL (dB)	d (mm)	References
CIP/SiO_2	9.6–11.2 GHz	−38.8	1.9	This work
CIP/MnO2	2–8 GHz	−39.1	3.5	[11]
Mixture of spherical and flaky CIP	10–12 GHz	−33	2	[7]
CIP/Carbon black	–	−17.5	1.5	[10]
Flaky CIP/SnO_2	–	−20.5	2.3	[15]

layer was prepared on the surface of CIP; the thickness of the coating layer increases with the increasing of the amount of TEOS. In the process of forming SiO_2 layer, the surface tensions of the interfaces between CIP and the solution, SiO_2 and the solution, CIP and SiO_2 result in the island-shaped distribution.

3.2. Absorbing mechanism analysis

Complex permittivity ($\varepsilon_r = \varepsilon' - j\varepsilon''$) and complex permeability ($\mu_r = \mu' - j\mu''$) can determine the absorption properties of a material. The complex permittivity and permeability of the powder samples/paraffin composite ($x=2$, 3, 4 and 8) were measured in

the frequency range of 1–18 GHz and shown in the Fig.4. When the value of x is 2 or 3, there are considerable increases in the real part of permittivity due to the SiO_2coating. This phenomenon can be explained by Maxwell–Wagner mechanism [20]. Improvements on both real parts and imaginary parts (at most wavebands in 1–18 GHz) of complex permeability can also be observed from Fig.4. But both complex permittivity and permeability declined to the level of uncoated CIP as x increases. In the following discussion the microwave absorbing mechanism of $x=2$ and $x=3$ will be the focus.

The tangents of loss angles can be calculated by the following equations:

$$\tan \delta_{\varepsilon} = \frac{\varepsilon''}{\varepsilon'}$$

$$\tan \delta_{\mu} = \frac{\mu''}{\mu'}$$

The tangents of loss angles can reflect the mechanism of EM wave loss. By the curves in Fig.5, it is obvious that all coated samples are magnetic loss type absorber in the waveband of 1–18 GHz. Generally speaking, there are two sorts of mechanisms which are involved in high-frequency magnetic loss: current eddy loss and natural resonance. The following expression is tenable, if the diameter of metal particles is less than the skin depth (10–30 μm for CIP, depends on frequency):

$$\frac{\mu''}{\mu'} \propto \frac{\mu' f D^2}{\rho}$$

Where F is the frequency of EM wave, ρ is the electrical resistivity of metal particles.

If the magnetic loss only results from the eddy current loss, the values of $f^{-1}(\mu')^{-2}\mu''$ should be constant [21]. The curve in Fig.6 shows the variation of the value of $f^{-1}(\mu')^{-2}\mu''$ versus frequency. It is shown that in the ranges of 4–10 GHz and 15–18 GHz the curve of coated CIP ($x=3$) has a relatively small slope, which means current eddy loss plays a more important role in these ranges. The slope of the curve changed massively and sharply around 13 GHz where CIP without treatment only has a small one. This peak also related to the magnetic loss peak in Fig.5 at the same waveband. Since this peak appeared at a certain frequency, it was caused by natural resonance. The coating layer has enhanced the strength of this natural resonance.

3.3. Absorption properties

In this paper, we use reflection loss (RL) to measure the properties of samples. According to the transmission line theory, the RL of normal incident electromagnetic wave can be calculated from the complex permittivity and complex permeability at a given frequency and thickness of microwave absorbing materials. For a single-layer absorber, the reflection loss can be calculated based on the following equations:

$$RL = 20 \log|\Gamma|$$

$$\Gamma = \frac{(Z-1)}{(Z+1)}$$

$$Z = \sqrt{\frac{\mu_r}{\varepsilon_r}} \tan h\left\{ j\frac{2\pi f d}{c}\sqrt{\varepsilon_r \mu_r} \right\}$$

Where Z is the input impedance of the absorber, ε_r and μ_r are the complex relative magnetic permeability and dielectric permittivity of the samples, respectively, f is the frequency of microwaves, d is the thickness of an absorber, c is speed of light.

Fig.7(a) shows the results of the calculations. It can be seen that the minimum of RL reaches −38.8 dB at 10.4 GHz when $d=1.9$ mm, and the RL exceeding −10 dB (over 90% EM wave absorption) can be observed from 8 GHz to 14 GHz, and RL exceeding −20 dB can be observed from 9.6 GHz to 11.2 GHz. Both the depth and width of RL are improved in coated sample, when contrast with uncoated CIP samples. It can also be seen that the peaks of samples with different additional amount shifted from 7 GHz to 13 GHz when $d=1.9$ mm. The minimum of peaks changed from −38.8 dB to −18.9 dB. So it is possible to control the absorption peak by changing the additional amount of a sample.

Table 1 shows EM absorption properties of some recent reports. To compare with other absorbers, the coating layer may bring CIP improved anti-acidic characteristics [22]. What is more, the whole preparation process is under air atmosphere, and all materials used in this experiment are easy to purchase, these can bring SiO_2-CIP coating absorber an advantage in practical production.

4. Conclusion

By the method mentioned in this paper, SiO_2-layers can be successfully prepared on the surface of CIP. The thickness of the layer was 5–10 nm approximately. The absorption abilities of coated samples were mainly from magnetic loss. The current eddy loss and the natural resonance both affected in the magnetic loss, the introducing of coating layer enhanced the natural resonance. The band width and depth of RL were improved by introducing the SiO_2 layers. The coated samples showed excellent absorption properties, the position of absorption peak by changing the additional amount of a sample.

Acknowledgment

This project is supported by the National Natural Science Foundation of China (No. 11264023) and the Education Department of Gansu Province (No. 1210ZTC035). J. Li would like to thank D.M. Tang for his help of the measurements.

References

[1] Y. Liu, X.X. Liu, X.J. Wang, Double-layer microwave absorber based on $CoFe_2O_4$ ferrite and carbonyl iron composites, J. Alloys Compd. 584 (2014) 249–253.
[2] G.J.H. Melvin1, Q.-Q. Ni, Y. Suzuki, T. Natsuki, Microwave-absorbing properties of silver nanoparticle/carbon nanotube hybrid nanocomposites, J. Mater. Sci. 49 (14) (2014) 5199–5207.
[3] S. Vinayasree, M.A. Soloman, Vijutha Sunny, P. Mohanan, Flexible microwave absorbers based on barium hexaferrite, carbon black, and nitrile rubber for 2–12 GHz applications, J. Appl. Phys. 116 (2014) 024902–024902-7.
[4] K.K. Gupta, S.M. Abbas, T.H. Goswami, A.C. Abhyankar, Microwave absorption in X and Ku band frequency of cotton fabric coated with Ni–Zn ferrite and carbon formulation in polyurethane matrix, J. Magn. Magn. Mater. 362 (2014) 216–225.
[5] S. Kimura, T. Kato, T. Hyodo, Electromagnetic wave absorption properties of carbonyl iron-ferrite/ PMMA composites fabricated by hybridization method, J. Magn. Magn. Mater. 312 (2007) 181–186.
[6] Z.J. Song, L.J. Deng, J.L. Xie, Synthesis, dielectric, and microwave absorption properties of flake carbonyl iron particles coated with nanostructure polymer, Surf. Interface Anal. 46 (2) (2014) 77–82.
[7] J.H. He, W. Wang, A.M. Wang, Electromagnetic parameters and microwave-absorption properties for the mixtures of mechanically milled spherical and flaky carbonyl iron powders, Acta Metall. Sin. 25 (3) (2012) 201–206.
[8] C.L. Yin, J.M. Fan, L.Y. Bai, Microwave absorption and anti-oxidation properties of flaky carbonyl iron passivated with carbon dioxide, J. Magn. Magn. Mater. 340 (2013) 65–69.
[9] Y.H. Zou, Y.J. Qing, L.Y. Jiang, Improved microwave absorption of carbonyl iron powder by the array of subwavelength metallic cut wires, IEEE J. Elect. Top. Quant. Electron. 16 (2010) 441–445.
[10] L.D. Liu, Y.P. Duan, L.X. Ma, Microwave absorption properties of a wave-absorbing coating employing carbonyl-iron powder and carbon black, Appl. Surf.

Sci. 257 (2010) 842–846.
[11] W.Q. Zhang, S.W. Bie, H.C. Chen, Electromagnetic and microwave absorption properties of carbonyl iron/MnO_2 composite, J. Magn. Magn. Mater. 358 (2014) 1–4.
[12] X. Li, Y. Zhang, J. Chen, Composite coatings reinforced with carbonyl iron nanoparticles: preparation and microwave absorbing properties, Mater. Technol. 29 (1) (2014) 57–64.
[13] Y.C. Qing, W.C. Zhou, S. Jia, Electromagnetic and microwave absorption properties of carbonyl iron and carbon fiber filled epoxy/silicone resin coatings, Appl. Phys. A 100 (2010) 1177–1181.
[14] X.W. Ji, M. Lu, F. Ye, Preparation and research on the electromagnetic wave absorbing coating with Co-ferrite and carbonyl iron particles, J. Mater. Sci. Res. 2 (2) (2013) 35–40.
[15] X.B. Wu, H.L. Luo, Y.Z. Wan, Preparation of SnO_2-coated carbonyl iron flaky composites with enhanced microwave absorption properties, Mater. Lett. 93 (2013) 139–142.
[16] Y.B. Zhu, Y.C. QING, S. JIA, Microwave absorbing properties of SiO_2 coated carbonyl iron particles, Mater. Rev. 2 (2010) 9.
[17] G.X. Tong, W. Wang, J.G. Guan, Properties of Fe/SiO_2 core–shell composite particles with different nanoshell thickness, J. Inorg. Mater. 21 (6) (2006) 1461–1466.
[18] A.K. Li, L.Y. Li, L.W. Wu, J.H. Yi, Preparation of $Fe_{85}Si_{9.6}Al_{5.4}$ soft magnetic composite powder with silica insulation coating by sol–gel method, Chin. J. Nonferr. Met. 23 (4) (2013) 1065–1072.
[19] H.S. Chen, Z.Y. Sue, J.C. Shao, Investigation on FT-IR spectroscopy for eight different sources of SiO, Bull. Chin. Ceram. Soc. 30 (4) (2011) 934–937.
[20] L.B. Li, F.Z. Huang, X.M. Lu, J.S. Zhu., Maxwell—Wagner mechanism induced dielectric relaxation in $BiFeO_3/Bi_{3.25}La_{0.75}Ti_3O_{12}$ film, Integr. Ferroelectr. 110 (2009) 25–33.
[21] L. Wang, F. He, Y.Z. Wan, Facile synthesis and electromagnetic wave absorption properties of magnetic carbon fiber coated with Fe-Co alloy by electroplating, J. Alloys Compd. 509 (2011) 4726–4730.
[22] Y.C. Qing, W.H. Zhou, S. Jia, Microwave electromagnetic property of SiO_2-coated carbonyl iron particles with higher oxidation resistance, Phys. B: Condens. Matter 406 (4) (2011) 777–784.